

# Snap-through of a bistable beam using piezoelectric actuation

Taha Ajnada<sup>1</sup>, Yves Bernard<sup>2,3</sup> and Laurent Daniel<sup>2,3</sup>

**Abstract**—The paper presents the snap-through of a bistable system using piezoelectric (PZ) actuation. The bistable system consists of a pre-buckled beam fixed between two jaws. The bistability and snap-through of the beam are modelled using two approaches. An analytical model is first implemented. The results are compared to a full finite element simulation. These modelling approaches are used to find the optimal positioning of the PZ patches used for switching. The PZ-actuated snap-through is then modelled using both an analytical equivalent moment model and finite element simulations. An experimental validation setup is developed accordingly. The validation addresses all aspects of the modelling : bistability, snap-through and PZ-actuated snap-through. For the latter two configurations were studied, namely a switching actuated by a single PZ patch or by two patches. A remarkable agreement is found between both modelling approaches and experimental measurements. The proposed analytical modelling tool can be used for rapid pre-design of bistable devices. It is for instance shown that a centimeter-scale steel-device with an initial transverse displacement about 1 mm can be switched with a few-Newton force or alternatively with a few hundreds of Volts using a PZ patch.

**keywords:** Bistable systems, piezoelectric actuation, buckled beam

## I INTRODUCTION

Bistable systems exhibiting two equilibrium states separated by an unstable transition region [1] are the simplest illustration of multistable systems. Systems that exploit buckling are promising for bistability application, notably because they are easy to realise and can be two-dimensional. A buckled beam can switch from an up-position to a down-position, and vice-versa. This switching is called snap-through [2][3]. It can take place under purely mechanical action, as well as through thermal, electrical or other stimuli.

Several techniques exist to obtain a uniform curvature after buckling [4].

Bistable systems are used in many applications such as switches [5][6][7], microgrippers in microbots [8][9], or haptic feedback devices [10]. Vibrational energy harvesting is also one of the applications of bistable buckled systems [11]. Bio inspired robots like trap-jaw ants as well as origami robots that detect, decide and react use bistability

This work was supported by the Automotive Mechatronics Chair, a cooperation between Faurecia, CentraleSupélec and Esigelec.

<sup>1</sup>Univ. Lille, Arts et Metiers Institute of Technology, Centrale Lille, Junia, ULR 2697 - L2EP, F-59000 Lille, France

<sup>2</sup>Université Paris-Saclay, CentraleSupélec, CNRS, Laboratoire de Génie Electrique et Electronique de Paris, 91192, Gif-sur-Yvette, France

<sup>3</sup>Sorbonne Université, CNRS, Laboratoire de Génie Electrique et Electronique de Paris, 75252, Paris, France

principle [12][13]. Bistability is also used with metamaterial to fabricate stable mechanical memories [14].

A structure can buckle and give a bistable system, just as the system can be bistable by design [15].

PZ materials can be interesting candidates to switch bistable systems. The use of PZ materials, e.g., in small displacements generation applications (under high voltage levels), leads to good controllability of the actuators and high resolution, reaching the nanoscale [16], with very fast response times. The electromechanical conversion is increasingly improved nowadays [17]. It takes place silently and with a negligible magnetic field (compared to conventional electromagnetic solutions). Operation at cryogenic temperatures is possible even if the performance of the actuators is lower at low temperatures. PZ materials can operate at high temperatures without failure. Their usage temperature range is limited though by their Curie point  $T_C$ , about  $160^\circ\text{C} - 350^\circ\text{C}$  for ferroelectric ceramics [18]. The lifetime of these materials is relatively high, with very low consumption, especially in static use [19].

PZ materials bounded to a buckled beam can be used to operate the bistable system, which switches from one stable state to another [20][21]. An advantage of this approach is to create large displacements (buckling) from small piezoelectric strains.

Different types of piezoelectric materials, such as ceramics, micro-fiber composites or polymers can be used to actuate passive structures [22].

This paper investigates the design of a bistable system actuated by PZ actuators, and not just with an external punctual effort without discussing its source [23].

In a first part, the governing equations for the buckling of a beam are recalled. Then, the snap-through under the action of a force is modelled and the results are validated using a dedicated experimental setup. Finally, the snap-through under the PZ actuation is modelled and the results are similarly validated using a dedicated experimental setup.

## II BUCKLED BEAM

Buckling is an abrupt appearance of a change in shape in a direction different from that of the applied loads. Buckling often leads to the ruin of structures. However, it can be used to dissipate energy, or create very flexible structures [24][25]. This phenomenon is an instability because it contains an unstable equilibrium, and is difficult to predict because it is very sensitive to geometric or material imperfections, and to boundary conditions.

The aim of this first part is to study in detail a bistable structure consisting in an axially compressed and buckled single beam, with a view to use it later under piezoelectric actuation. The purpose is to demonstrate that first, this chosen system is bistable and then characterise it mechanically to understand its properties and the levels and location of forces that need to be applied to exploit its bistability.

In order to obtain a buckled beam, a basic configuration is a double built-in elastic beam. The beam has one end fixed, the other end can move axially (along x axis) under the effect of a force. An axial force  $P$  is applied to the movable end. This leads to the displacement  $\delta$  of this extremity, and consequently the appearance of a transverse displacement  $D$  when  $P$  exceeds a threshold value. Once the desired displacement  $D_0$  is obtained, the supporting device is fixed.

The default set of parameters in this section for the numeric applications in analytical modelling, finite element modelling (FEM) and experiments are summarised in table I.

Beam Parameter	Unit	Value
Young modulus $E_b$	GPa	210
Thickness $t_b$	mm	0.3
Length $l_b$	mm	50
Width $b$	mm	10

**TABLE I:** Dimensions and material parameters used for the FEM of the beam buckling and bistability study. The parameters are shown in Figure 1.  $b$  is the beam width in the space third dimension (not shown in the figure)

### II-A Analytical modelling

The entire study is conducted in accordance with the fundamental assumptions of beam theory. First, Saint-Venant principle is considered: the results are valid only at a sufficiently large distance from the region of application of the external mechanical actions. Second, according to the Navier-Bernoulli hypothesis, the sections normal to the mean line remain flat and normal to the mean line during deformation.

The extremity axial displacement  $\delta$  can be decomposed into two parts ( $\delta = \delta_e + \delta_b$ ):  $\delta_e$  related to the elasticity of the beam and  $\delta_b$  which generates the central deflection  $D$ . The critical axial force, at which the transverse displacement appears, and corresponding to the critical value  $\delta_e^{\text{crit}}$ , is denoted by  $P^{\text{crit}}$ :

$$P^{\text{crit}} = k \cdot \delta_e^{\text{crit}} \simeq \frac{A_b E_b}{L_b} \delta_e^{\text{crit}} \quad (1)$$

where  $k \simeq \frac{A_b E_b}{L_b}$  is the beam stiffness constant ( $N.m^{-1}$ ),  $A_b = b t_b$  the section ( $m^2$ ),  $E_b$  the Young Modulus (Pa) and

$L_b = l_b + \delta$  the initial length ( $m$ ) of the beam.

The various variables involved are (Figure 1) : axial force  $P$ , axial displacement  $\delta$  and central displacement  $D$ . The study hypotheses are:

- small displacements with regard to the length of the beam  $\frac{D}{L_b} \ll 1$
- elastic behaviour of materials
- $(C_1 C_2)$  part of the beam after buckling is a sine branch
- only the first buckling mode appears

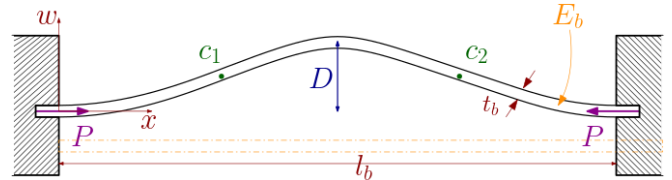


**Fig. 1:** 2D buckled structure (length  $l_b$ , width  $b$ , thickness  $t_b$  and Young modulus  $E_b$ ). The axial force  $P$  allows to reach an initial transverse displacement

Figure 1 shows a 2D view of the buckled system after axial compression, with the addition of the thickness  $t_b$  and the material parameter  $E_b$  of the beam.

The expression of  $P^{\text{crit}}$  as a function of beam parameters is demonstrated by Timoshenko [26]:

$$P^{\text{crit}} = 4\pi^2 \frac{E_b I}{L_b^2} \quad (2)$$

and  $\delta_b$ , the quantity responsible for the appearance of the transverse displacement  $D$  is given by:

$$\delta_b = \frac{\pi^2 D^2}{4L_b} \quad (3)$$

Figure 2 shows the transverse displacement  $D$  as a function of the axial displacement with its two components  $\delta = \delta_e + \delta_b$ . First, the focus is only on the analytical curve.

For the low values of  $\delta$  (less than  $15 \mu m$ ), the transverse displacement is zero. There is no buckling. This is the linear behaviour of the beam, which is characterised by its stiffness and  $P^{\text{crit}}$ . Continuing to compress axially the moving end, any desired transverse displacement, respecting the system's geometric dimensions, is achieved. One (arbitrary) choice is to stop around  $D_0 = 1 \text{ mm}$ . This value serves as a reference point.

### II-B Finite element modelling

To validate the analytical result, a post-buckling study with the numerical modelling code Comsol under the plane stress assumption is conducted. A simple beam with one end clamped is axially compressed by moving the end that is free to move. The compression is either by applying

an axial force or by applying an axial displacement. Both approaches lead to the same result. When using an elasticity package, the beam has a linear and elastic behaviour. No transverse deformation appears with axial compression. This is due to the symmetry of the stresses in the beam section. The stress symmetry needs to be broken so that the transverse displacement occurs, i.e., so that the beam buckles. A method is to apply a very small transverse force (of the order of 0.1 N) at the middle of the beam, so that it breaks the stress symmetry. It has been verified that the value of this transverse force is small enough not to influence the final result, i.e., the axial force, the corresponding transverse displacement and the strain levels. The domain was discretised using triangular mesh elements using cubic Lagrange shape functions. The structure is simple. The meshing sequence contains only global size nodes.

### II-C Experimental validation

To validate the model of transverse displacement as a function of axial displacement, a buckling experiment is carried out on a double-clamped beam, actuated with an axial force to make it buckle.

For measurements, Keyence sensor and its conditioning circuit LK-G3000, are used. A sensor head (LK-G152) is used to measure the vertical displacement  $D$  at the middle of the beam. Another sensor head (LK-G10) is used to measure the axial displacement on the edge of the linear translation stage. this displacement is assimilated to  $\delta$  (Figure 3).

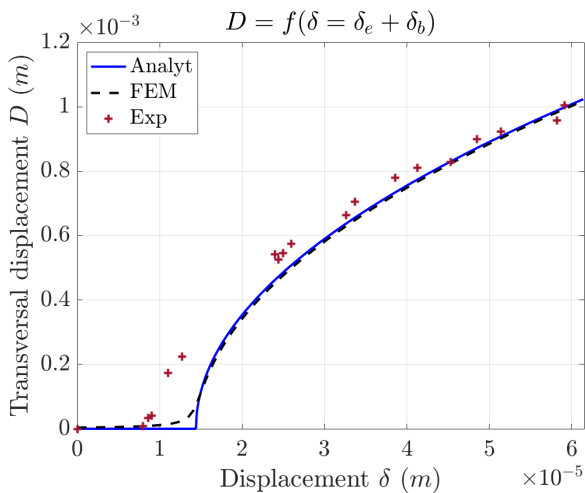


**Fig. 2:** Analytical, FEM and experiment results for the transverse displacement  $D$  as a function of the axial displacement  $\delta$

Based on this, the  $(D = f(\delta))$  curves obtained from the analytical and numerical models are plotted in figure 2. The experimental measurements are also shown (symbols). It can be seen that the two modelling curves have the same shape.

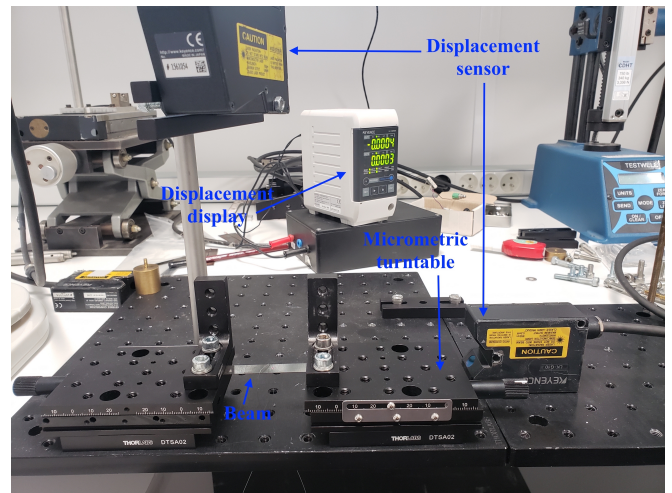


**Fig. 3:** Clamped beam test bench with two laser sensors to measure axial imposed displacement  $\delta$  and transverse induced displacement  $D$

The numerical curve shows a transverse displacement earlier than the analytical approach. This is mainly due to the small transverse force which breaks the symmetry and favours early buckling.

The experimental result also shows good agreement with the two models. In the region where buckling is clear ( $\delta > 20 \mu\text{m}$ ), a maximum relative error of 13% is observed. The onset of buckling starts earlier in the experiments compared to the models. Geometric and material imperfections are partly responsible for this difference. The difference with the model is also due to the equipment used to clamp the beam and then apply the axial force. The test bench should be infinitely rigid, but it is not precisely the case.

Now with the buckled structure, all ends are fixed and the resulting displacement  $D_0 \simeq 1 \text{ mm}$  is then maintained. The effect of a transverse force  $2R$  on the beam displacement  $D$  will be modelled.

## III BISTABILITY

The structure in Figure 4 under the action of external axial and transverse forces is considered.

### III-A Analytical modelling of bistability

Solving the buckling problem can be reduced to solving a Sturm-Liouville problem. The eigenvalues resulting from solving this problem give rise to non-trivial eigenfunctions [27][28]:

$$w_i(x) = \begin{cases} C_i (1 - \cos(n_i x)) & \text{if } i \in \{0, 2, 4, \dots\} \\ C_i \left( 1 - \cos(n_i x) - \frac{2}{n_i l_b} (n_i x - \sin(n_i x)) \right) & \text{if } i \in \{1, 3, 5, \dots\} \end{cases} \quad (4)$$



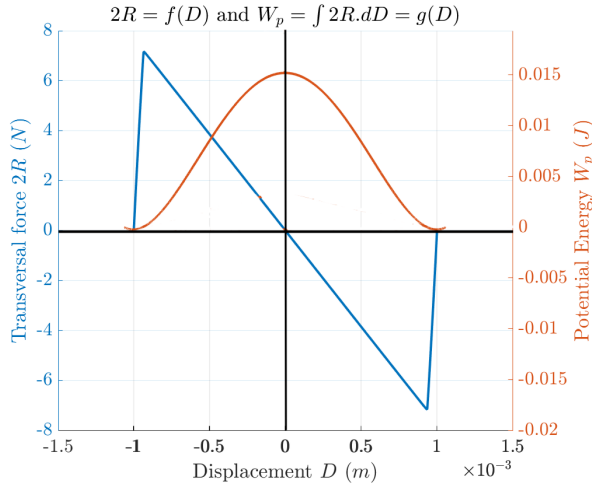


**Fig. 5:** Transverse force  $2R$  and potential energy related to this force  $2R$  versus transverse displacement  $D$  for a buckled beam

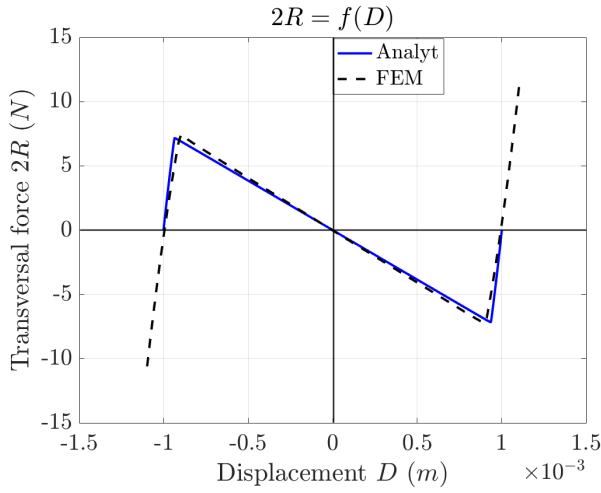


**Fig. 6:** Analytical and FEM of snap-through process of a double clamped beam: transverse force  $2R$  as a function of transverse displacement  $D$  for initial displacement  $D_0 \pm 1mm$

Agreement between the results of the analytical model and those of the numerical model is noted. The results concern both types of snap-through, from bottom to top and from top to bottom. For the given dimensions, with  $D_0 = 1\text{ mm}$ , the switching force is around  $7\text{ N}$  and the displacement  $D$  when switching is around  $0.9\text{ mm}$ .

### III-C Experimental validation

An experimental study of buckling and mechanical actuation of the bistable system by a transverse force is conducted. The aim is to experimentally validate the bistability curve of the buckled steel beam.

The beam with the dimensions given in the introduction is compressed, between two jaws that can slide or be fixed. The beam is therefore axially compressed to buckling with

an initial midpoint deflection of  $D_0 \simeq 1\text{ mm}$ . From this initial configuration, a transverse force is applied step by step, using weights hanged in the middle of the beam. The evolution of the displacement  $D$  is measured using the laser sensor (see Figure 7). The curve of transverse force as a function of midpoint displacement  $2R = f(D)$  is then plotted.

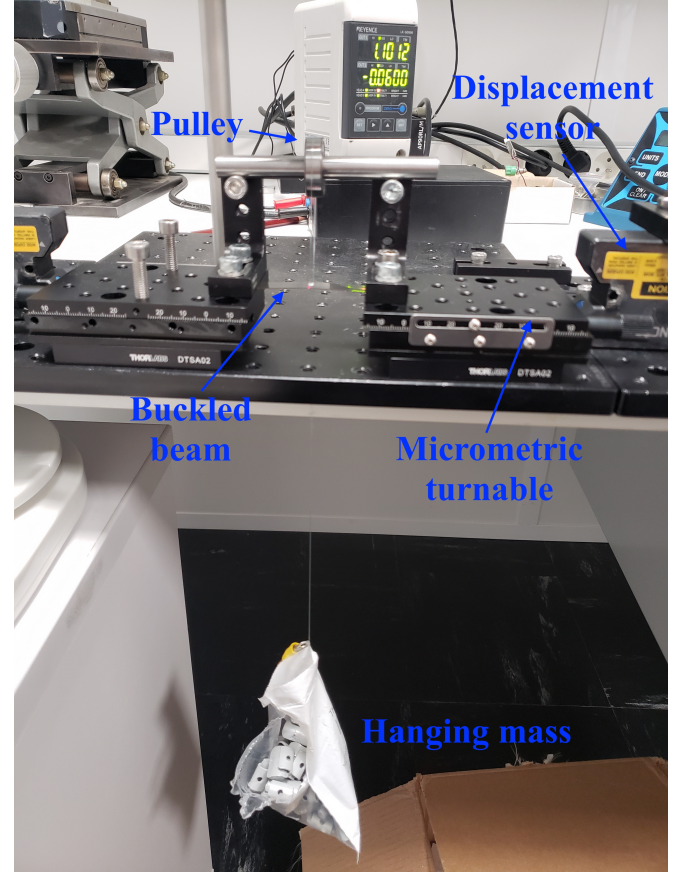


**Fig. 7:** Test bench for plotting transverse force  $2R$  versus transverse displacement  $D$ : force is applied by suspended masses and displacement is measured with the transverse laser sensor. The photo shows the case of snap-through from bottom to top, where an upward force is applied using a pulley

The experimental results of the tests carried out are shown with the model curve in Figure 8. Two series of measurements are shown. All other measurement series remain in the same region between these two.

The maximum force, i.e., the critical switching force, is lower than that predicted by the model (maximum relative error of 18% for an upward switching). This is due to the model's assumptions (isotropy and other mechanics of materials assumptions) and the rigidity of the axial compression system, assumed to be infinitely rigid. Also, the test has been repeated on a beam for different initial displacements  $D_0$ . For each test, the experiment was stopped when the applied transverse force led to the snap-through of the structure.

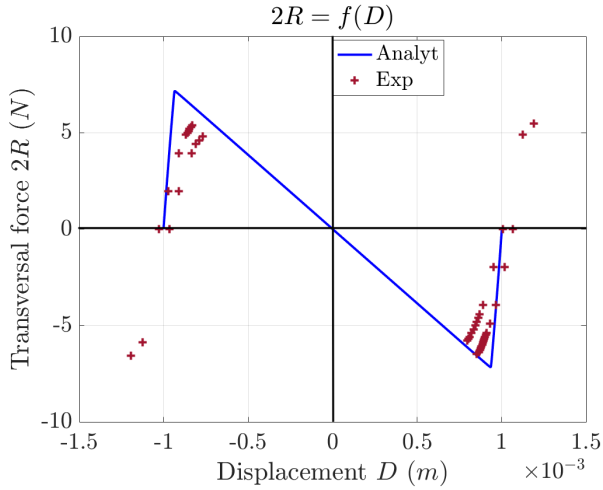


**Fig. 8:** Transverse force  $2R$  versus transverse displacement  $D$  for a buckled beam: comparison between modelling and experiment

Despite the concern for symmetry between the top and bottom positions of the buckled beam, Figure 9 shows consistency between the predictions of the analytical model  $2R = f(D)$  and experiment. The observed differences are mainly attributed to measurement errors and to some uncertainty concerning the boundary conditions at the jaws.

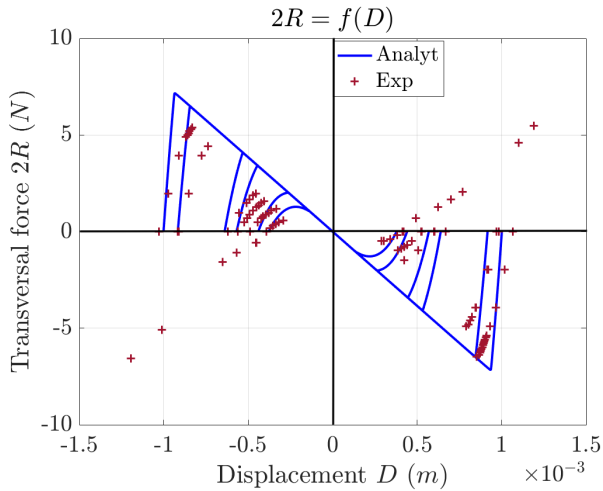


**Fig. 9:** Transverse force  $2R$  versus transverse displacement  $D$  for a buckled beam: theory and experiment for different values of initial displacement  $D_0$

The stop point of the measurements is the point of switching from the high state to the low state and vice versa. This is done instantaneously and the midpoint shift goes directly from a positive to a negative value or the opposite.

### III-D Conclusion

This part was dedicated to the characterisation of the buckled beam. First, a beam undergoes axial compression

and buckles. Buckling was modelled analytically, numerically and the models were validated experimentally. Then, from this deformed configuration, the impact of a transverse force was modelled and experimentally tested to ensure the results validity of the beam's response to transverse mechanical force, in particular the snap-through phenomenon. An order of magnitude can then be estimated on the level of force that needs to be applied, in particular cases of bistable beam thicknesses, to make it switch from one stable state to the other. This Force level depends on the initial displacement of the beam  $D_0$ .

## IV SNAP-THROUGH USING PZ ACTUATORS

The aim of this second part is to study analytically, by Finite Element Modelling (FEM) and experimentally the feasibility of switching a bistable system from one state to another using only piezoelectric (PZ) actuation. The purpose is to demonstrate that the equivalent moment models [31][32][33] are valid to replace the PZ actuation in the case of a buckled system by axial compression. An optimisation study will be conducted to minimise the required voltage to switch the structure from one stable state to the other, by adjusting the position of the PZ patch. This will be done analytically and by FEM. The comparison between the two results will serve to validate the use of equivalent actuation models (especially of moments) in this compression case, to understand and anticipate the snap-through of a bistable system. The interesting positions of the PZ patches on a bistable structure will be exploited to make an experimental prototype which will serve for validation.

The set of parameters used by default in this section for the numerical values in analytical modelling, finite element modelling (FEM) and experiments are summarised in table II.

	PZT	beam
Young modulus (Pa)	$E_p = 146 \cdot 10^9$	$E_b = 210 \cdot 10^9$
Poisson's ratio	/	$\nu_m = 0.33$
strain sensitivity (m/V)	$d_{31} = -62 \cdot 10^{-12}$	/
$l \cdot b \cdot t$ ( $mm^3$ )	$14 \cdot 14 \cdot 0.3$	$70 \cdot 14 \cdot 0.3$

**TABLE II:** Geometrical and material properties for the buckled beam with PZ actuation. Geometry:  $(l_p \cdot b \cdot t_p)$  for the PZT actuator and  $(l_b \cdot b \cdot t_b)$  for the beam

### IV-A Analytical modelling

The study is conducted in accordance with the fundamental assumptions of continuum Mechanics. The principle of Saint-Venant is considered. According to the Navier-Bernoulli hypothesis, the sections normal to the mean line remain flat and normal to the mean line during deformation. It is assumed that  $|w'| \ll 1$  for very small displacement, allowing to neglect the rotation angle after

deformation in the expression of the curvature.

This section addresses the case of the simple beam. It is a steel beam on which a PZ patch is perfectly bonded. In an experiment, the actuator is usually bonded to the structure via an adhesive. The experimental results show that increasing the adhesive thickness changes the electromechanical impedance and resonance frequency of the piezoelectric element, as well as the amplitude of the sensor signal [34]. For an actuator under the assumption of perfect bonding to the host structure, which is our study case, [32] showed that the shear stress between the actuator and the host beam was transferred mainly over an infinitesimal region at the actuator ends. This is consistent with the pin-moments models at the actuator ends that will be used.

When the system buckles and the desired displacement is reached, the ends are fixed. By supplying voltage to the PZ patch, it actuates the structure to allow switching from one stable equilibrium state to another.

With the equivalent moment approach, the study of the PZ actuation also amounts to a purely mechanical study. In the case of pure compression with an axial force  $P$  (see Figure 10), Euler-Bernoulli equation can be written as:

$$\frac{d^4 w}{dx^4} + \frac{P}{EI} \frac{d^2 w}{dx^2} = 0 \quad (11)$$

where  $EI$  is the stiffness of the system's part ( $E$  is Young modulus and  $I$  is the quadratic moment) which varies depending on whether it is the PZ patch bonding area or not.

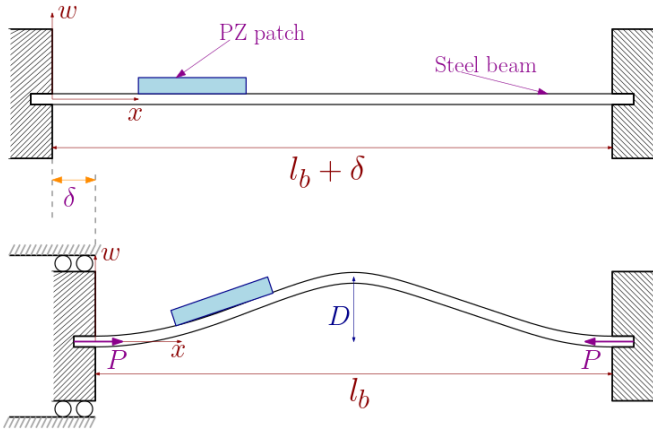


**Fig. 10:** Simple beam on which is bonded a PZ material: structure buckling to have the final configuration

#### IV-A.1 Solution if the buckled system is actuated by an external effort

For a compressed buckled beam actuated or by an external effort, the form of the deflection can be written analytically as a sum of the first and second modes (for buckling behaviour) with the addition of a particular solution (for equilibrium):

$$w(x) = w_1(x) + w_2(x) + w_p(x) \quad (12)$$

$w_1(x)$ ,  $w_2(x)$  and  $w_p(x)$  expressions contain the external efforts applied on the buckled system, whether it is a single force (referred to as "F"), one moment (referred to as "M"), two moments in two points of application (referred to as "MM"), four moments in four points of application (referred to as "4M") or other forms of loads [29][35].

#### IV-A.2 Analytical modelling of PZ actuation on a bistable beam using the equivalent moment approach

The action of a voltage-fed PZ patch can be modelled by either pin-forces or pin-moments [31][36]. The second equivalence was chosen because of its consistency with the numerical result [33]. The pin-moments are on both side of the ends of the PZ, around the same axis, in opposite directions (see Figure 11) and with equal module given by the formula:

$$M = bE_p (-K^f I_p + (K^e - 1 - z_n K^f) T - z_n (K^e - 1) t_p) \Lambda, \quad (\Lambda = d_{31} \frac{V_0}{t_p}) \quad (13)$$

where  $I_p = \frac{(\frac{t_b}{2} + t_p)^3 - (\frac{t_b}{2})^3}{3}$  and  $T = \frac{(\frac{t_b}{2} + t_p)^2 - (\frac{t_b}{2})^2}{2}$ , where  $z_n$  defines the neutral axis of the beam ( $z$  position where the strain  $\epsilon_b$  is zero):

$$z_n = \frac{E_p (t_p^2 + t_p t_b)}{2(E_b t_b + E_p t_p)} \quad (14)$$

and where

$$K^f = \frac{2}{t_b + t_p} \left( 1 - \frac{E_b E_p t_b^3 t_p + E_b^2 t_b^4 + E_p^2 t_p^4 + E_b E_p t_b t_p^3}{E_p^2 t_p^4 + E_b^2 t_b^4 + E_b E_p (4t_b^3 t_p + 6t_b^2 t_p^2 + 4t_b t_p^3)} \right)$$

$$K^e = \frac{t_p^4 + \frac{E_b}{E_p} t_b^3 t_p}{t_p^4 + \frac{E_b}{E_p} t_b^4 + \frac{E_b}{E_p} (4t_b^3 t_p + 6t_b^2 t_p^2 + 4t_b t_p^3)}$$

are introduced to simplify the moment formula.

The actuation with piezoelectric patch supplied with voltage is modelled by an internal double moment that actuates the system at the ends of the patch, with the patch kept passive. The study becomes a mechanical resolution of a bistable system driven by point moments (moment input example by Cleary *et al.* [37]).

The length of the PZT patch  $l_p$  gives the distance between the pin-moments. Under the small displacement assumption, it is assumed that  $x_2 = x_1 + l_p$ , where  $x_1$  and  $x_2$  are the positions of the beginning and the end of the PZ patch. With a constant PZ patch length  $l_p$ , changing the application position of the first moment means changing the position of the second moment as well. The middle position of the PZ

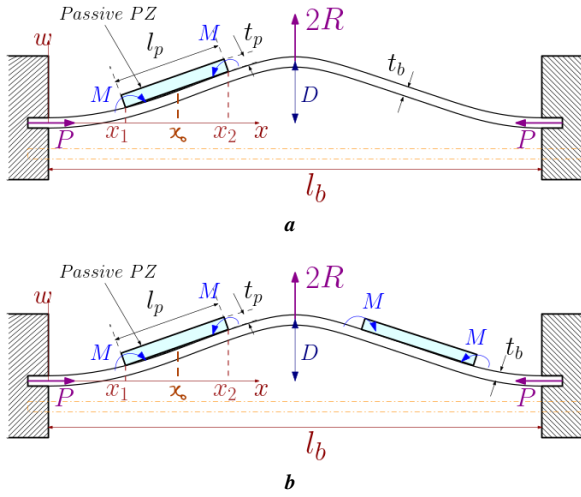


**Fig. 11:** Pin-moments equivalence with PZ actuation: (a) one PZ patch actuation and (b) two PZ patches actuation

patch  $x_0$  can be defined between  $x_1$  and  $x_2$  as a characteristic parameter of the PZ position.

Based on the configuration in Figure 11, the values of the applied moments on the bistable beam can vary, and the induced halfway point displacement is taken for each moment value. This allows drawing the moment-displacement curves and to get the values of moments needed for the snap-through of the beam. As the moments application position is changeable, its influence on the snap-through required moment may be quantified. This allows the plot of the critical snap-through curve that shows the snap-through moments as a function of the position of the moments. For one PZ actuation case, the shape of the analytical curve is given in Figure 12.

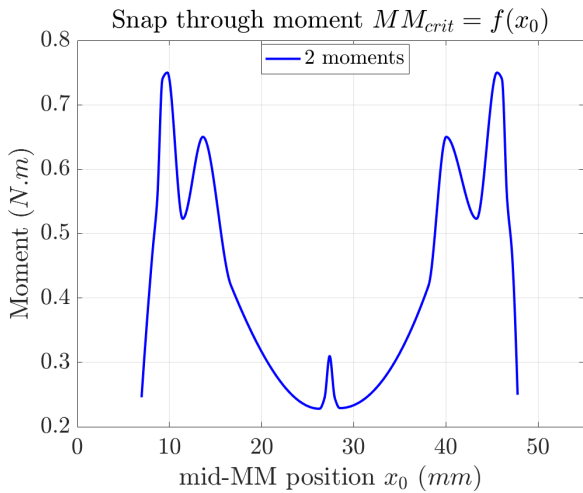


**Fig. 12:** Snap-through analytical curve: snap-through moment vs moment position

This curve of critical switching moments gives an idea of where two antagonist and  $l_p$  spaced moments should be applied for a low-effort snap-through. Two positions stand

out: close to the clamping bars or near the middle of the beam.

This analytical result will be compared with a numerical model where the beam is actuated with a voltage-supplied PZ patch. This will validate the accuracy of the moment model in this case of application and the snap-through model as well.

#### IV-B FEM of PZ actuation on a bistable beam

In the numerical study, the beam and a PZ actuator are perfectly bonded. One end of the PZ patch is at the  $x_1$  position, the other is at the  $x_2$  position. For each position, the system is first buckled by applying the axial force on its moving end. Then, the PZ actuator is supplied with voltage and the snap-through point is determined. Varying the position  $x_0$  of the middle of the PZ patch, the switching voltage as a function of the PZ position can be plotted. To compare this result with the analytical study conducted earlier, the moment-voltage equivalence given by equation (13) is used.

##### IV-B.1 One PZ actuator

The result of the comparison between the analytical model and the numerical model, concerning the snap-through voltage as a function of the actuator position, is given in Figure 13.

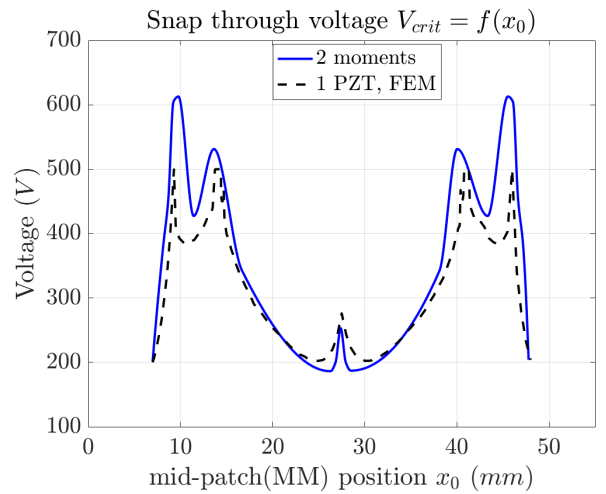


**Fig. 13:** Snap-through analytical and numerical curves: snap-through voltage vs PZ-patch/MM position

The two critical switching curves describe the same form of variation. Some errors between the two models appear in some regions, especially when the actuator is on two regions of the beam surface, one in extension and the other in compression. This is mainly due to all the simplifications of the Euler-Bernoulli model which does not take the shear stress into account.

The two best bonding positions for the PZ actuator to easily switch the bistable system stand out again: next to

the clamping bars and near the middle of the beam. The choice between these two can be made on the basis of the mechanical limit of the PZ patch. In the middle of the beam, it can be demonstrated that the strain at the common surface between the PZ patch and the beam is relatively large compared to the surface strain next to the clamping bars. There is therefore more interest in gluing the PZ actuator next to the clamping bars rather than near the middle of the beam.

#### IV-B.2 Two PZ actuators

The study is extended to the case of two PZ actuators whose positions are symmetrical using analytical and numerical modelling.

In the case of actuation with two PZs, it is considered for the analytical model that it happens as if the two antagonistic moments are applied at  $x_1$  and  $x_2$ , and two other moments are applied in the same way at  $x_3$  and  $x_4$ . Under the small displacement assumption, it is assumed that  $x_2 = x_1 + l_p$ ,  $x_3 = l_b - x_2$  and  $x_4 = x_3 + l_p$ . The result of the comparison between the analytical model (4 moments application) and the numerical model (2 PZ actuation), concerning the snap-through voltage as a function of the actuator position, is given in Figure 14.

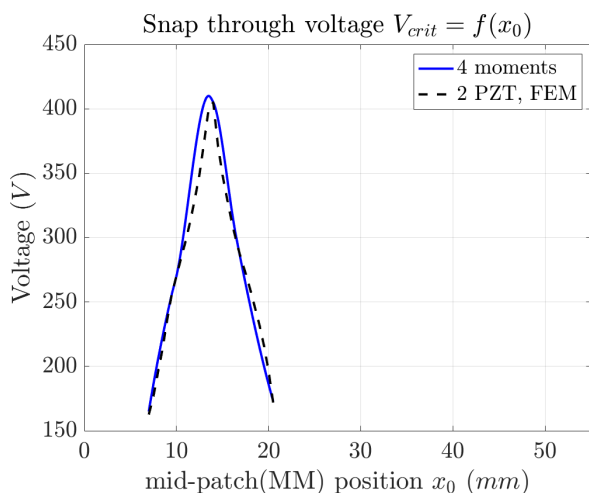


**Fig. 14:** Snap-through analytical and numerical curves in the case of two PZ actuators: snap-through voltage vs left PZ-patch/MM position

Actuation with two PZ patches offers interesting positions for switching with minimum supply voltage. These are almost the same as for a single PZ actuator. However, the voltage for switching with two PZ patches is lower. The voltage required for switching is about 25% less in the two actuators case.

### IV-C Experiment: snap-through using PZ actuators

#### IV-C.1 Prototyping

The chosen material for beams, which are bistable after

pre-stressing, is steel (XC75 steel). This choice is due to some studies carried out in the laboratory before [38]. They concluded that the shear force transfer between the PZT ceramics (NCE41) and the host structure is maximum, for these thickness dimensions range, when the structure is made of steel.

The nature of the surface is very important as it determines the quality of the bonding. It is therefore necessary to prepare the surfaces. The method used is that of surface preparation for the bonding of strain gauges. The first step is to polish and clean the surface: the PZ patch is gently polished at an angle of  $+45^\circ$  and  $-45^\circ$  with abrasive paper. The polished surface is cleaned with alcohol and degreaser and immediately wiped clean in one pass with a paper. Glue is added to the prepared surface and the PZ patch is placed on and tightened for more than eight hours to hold to the structure. The adhesive used is Araldite, a two component epoxy paste adhesive provided by Huntsman International LLC.

#### IV-C.2 Bistable beam actuated by PZ actuators

Numerical modelling of the PZ actuation of a bistable beam, using one PZT patch and two PZT patches, was carried out. Some positions optimising the snap-through voltage stood out. In particular, these points were tested experimentally for validation. Figure 15 shows the two cases of bonding one PZT actuator to a beam in an optimal position. Figure 16 shows the two cases of bonding two PZT actuators to a beam in an optimal position.

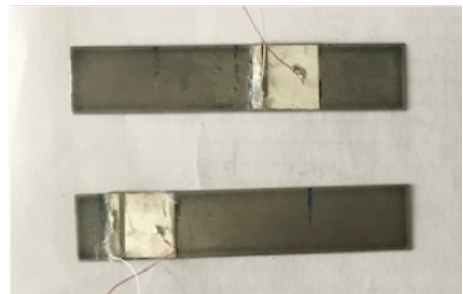


**Fig. 15:** Two cases of one PZT patch glued to a steel beam in two places that minimise the snap-through tension of the bistable beam system. Steel beam of (70, 14, 0.3 mm) and PZT patch of (14, 14, 0.3 mm)

The PZ patches are then supplied with voltage, with twenty volt jumps. This allows an overview of the timing and measurement of the snap-through voltage from one stable state to another. This is repeated with different voltage starting points, allowing error bars to be drawn on the voltage. The possibility to clamp the beam at different points allows testing a few points (voltage, position), around the optimal points.

An error on the position of the PZ patch of 1 mm is added. Figures 17 and 18 show the numerical result of the snap-through voltage curves as a function of the position of the PZ patches, together with some experimentally tested points.

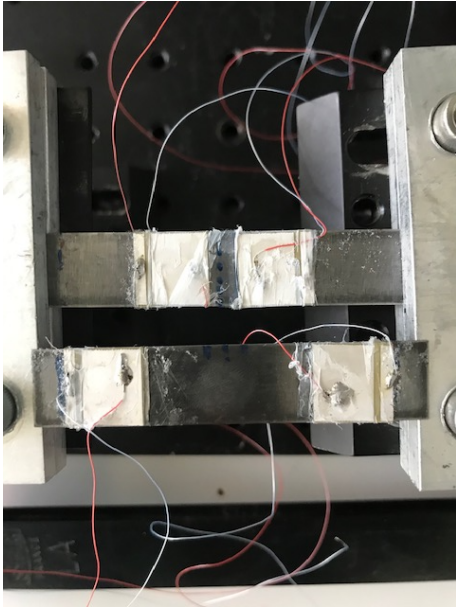


**Fig. 16:** Two cases of two PZT patches glued to a steel beam in two places that minimise the snap-through tension of the bistable beam system. Steel beam of (70, 14, 0.3 mm) and PZT patch of (14, 14, 0.3 mm)

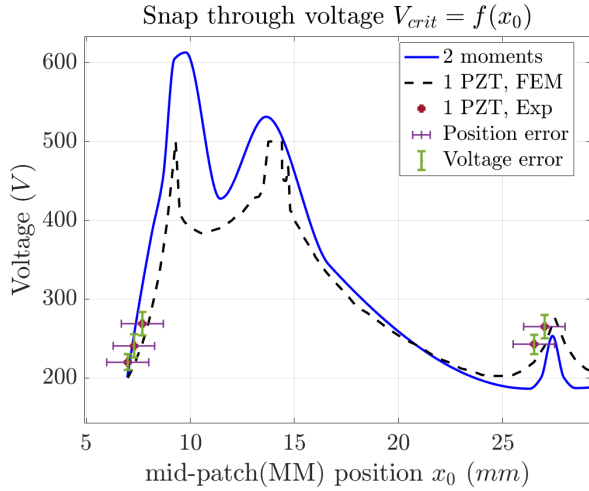


**Fig. 17:** Snap-through numerical curve with several experimentally validated points: snap-through voltage vs 1 PZT patch position

As shown in Figure 17, the numerical switching voltage is in the margin of error of the measured one. The adhesive layer between the PZT and the beam, used in the test bench and not taken into account in the model, is a source of error just as the mechanical boundary conditions.

In the case of two PZT patches bonded to the steel beam, the tolerance in the clamped area allows to test the switching for actuators positions (2 points close to the edges and 2 points close to the middle).

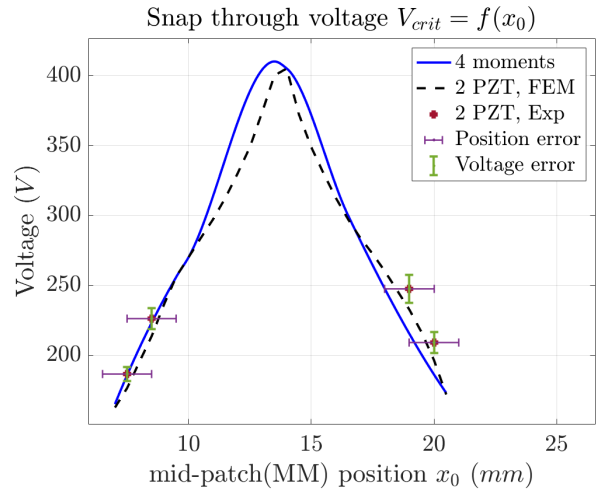


**Fig. 18:** Snap-through numerical curve with several experimentally validated points: snap-through voltage vs 2 PZT patches position

As shown in Figure 18, the numerical switching voltage is also in the margin of error of the measured one. For the same reasons as the single PZ patch case, the errors are explained by the sensitivity of the snap-through point to boundary conditions and the used equipment. The adhesive layer is a source of error here too.

#### IV-D Conclusion

The analysis carried out in this section provided an opportunity to discuss the operating principle of a bistable system snap-through under PZ actuation. It requires mechanical analysis of the buckling phenomenon, modelling of the actuation by piezoelectric materials and experimental validation work. This led to models validation by experimental approach, based on the buckled bistable beam actuated by PZ patches.

With the chosen deflection level ( $D_0 = 1$  mm), the PZT patches have indeed demonstrated their ability to switch a bistable buckled beam. This was proven for the steel beam of dimensions (70, 14, 0.3 mm) with PZT patches of dimensions (14, 14, 0.3 mm) glued on. An optimisation study was carried out to minimise the voltage required at snap-through as a function of the position of a single PZ patch and then that of two PZ patches. The characteristic points of this study were verified experimentally, and the errors were relatively small compared to the models.

## V CONCLUSION

Buckled beams are systems that can exhibit bistable behaviour. This study aimed to model and verify experimentally the snap-through of a bistable beam actuated with piezoelectric materials. After the analysis carried out along this work, the following conclusions can be drawn:

- 1) Using the proposed modelling approach, the dimensions and material properties of the beam allow to

predict whether the structure is bistable or not, the required level of axial force required for buckling and the level of transverse force then required for snap-through.

- 2) The comparison of the PZ actuation models concluded on the validity of the equivalent moment model with a relative error of the order of a few percents compared to the numerical model.
- 3) The switching from one stable state to the other using the PZ patches was demonstrated. Modelling was first used to define optimal position for PZ patches and an experimental prototype was then developed accordingly to validate the results.
- 4) The analytical model shows consistency with the numerical model, especially in regions that minimise the snap-through voltage. The experimental validation shows a good agreement with the models as well.

The full modelling approach can be used to design bistable devices with a large range of switching energies. It can also serve to use PZ patch as a mean to adapt to the possible variation in switching energy, for instance due to thermal dilatation, assembly uncertainties or manufacturing variability.

#### REFERENCES

- [1] Ryan L. Harne and K.W. Wang. *Harnessing Bistable Structural Dynamics: For Vibration Control, Energy Harvesting and Sensing*. John Wiley Sons Ltd, 2017.
- [2] Y. Yang and C. J. Kim. Testing and characterization of a bistable snapping microactuator based on thermo-mechanical analysis. *Proc. SolidState Sensors Actuators*, pages 337–340, 1995.
- [3] B. Wagner, H. Quenzer, S. Hoerschelmann, T. Lisek, and M. Juerss. Bistable microvalve with pneumatically coupled membranes. *Proc. IEEE MEMS*, pages 384–388, 1996.
- [4] Marie-Laure Dano, Mathilde Jean-St-Laurent, and Adam Fecteau. Morphing of bistable composite laminates using distributed piezoelectric actuators. *Smart Materials Research*, 2012, 2012.
- [5] C. Joshitha and B.S. Sreeja. Design and analysis of bistable mems switch. In *International Conference on Information Communication and Embedded Systems (ICICES2014)*, pages 1–4, 2014.
- [6] Y. Yang and C. J. Kim. A bistable snapping microactuator and its mechanical analysis. 12 1995.
- [7] Martin Hoffmann, Peter Kopka, and Edgar Voges. Bistable micromechanical fiber-optic switches on silicon with thermal actuators. *Sensors and Actuators A: Physical*, 78(1):28–35, 1999.
- [8] Zheng Zhang, Yang Li, Xiaochen Yu, Xianghao Li, Helong Wu, Huaping Wu, Shaofei Jiang, and Guozhong Chai. Bistable morphing composite structures: A review. *Thin-Walled Structures*, 142:74–97, 2019.
- [9] Zheng Zhang, Xianghao Li, Xiaochen Yu, Hao Chai, Yang Li, Huaping Wu, and Shaofei Jiang. Magnetic actuation bionic robotic gripper with bistable morphing structure. *Composite Structures*, 229:111422, 2019.
- [10] Roman Vitushinsky, Sam Schmitz, and Alfred Ludwig. Bistable thin-film shape memory actuators for applications in tactile displays. *Journal of Microelectromechanical Systems*, 18(1):186–194, 2009.
- [11] B. Andò, S. Baglio, A.R. Bulsara, and V. Marletta. A bistable buckled beam based approach for vibrational energy harvesting. *Sensors and Actuators A: Physical*, 211:153–161, 2014.
- [12] Yuzhe Wang, Qiong Wang, Mingchao Liu, Yimeng Qin, Liuyang Cheng, Ophelia Bolmin, Marianne Alleyne, Aimy Wissa, Ray H Baughman, Dominic Vella, et al. Insect-scale jumping robots enabled by a dynamic buckling cascade. *Proceedings of the National Academy of Sciences*, 120(5):e2210651120, 2023.
- [13] Wenzhong Yan, Shuguang Li, Mauricio Deguchi, Zhaoliang Zheng, Daniela Rus, and Ankur Mehta. Origami-based integration of robots that sense, decide, and respond. *Nature Communications*, 14(1):1553, 2023.
- [14] Tian Chen, Mark Pauly, and Pedro M Reis. A reprogrammable mechanical metamaterial with stable memory. *Nature*, 589(7842):386–390, 2021.
- [15] Marc R Schultz. A concept for airfoil-like active bistable twisting structures. *Journal of Intelligent Material Systems and Structures*, 19(2):157–169, 2008.
- [16] Yunlai Shi, Chengshu Lou, and Jun Zhang. Investigation on a linear piezoelectric actuator based on stick-slip/scan excitation. *Actuators 2021*, 10(39):1–12, 2021.
- [17] Stephen C. Thompson, Richard J. Meyer, and Douglas C. Markley. Performance of tonpilz transducers with segmented piezoelectric stacks using materials with high electromechanical coupling coefficient. *Acoustical Society of America*, 135(1):155–164, 2014.
- [18] Zhang Shujun and Yu Fapeng. Piezoelectric materials for high temperature sensors. *The American Ceramic Society*, 94:3153–3170, 2011.
- [19] R. Salazar, K. Larkin, and A. Abdelkefi. Piezoelectric property degradation and cracking impacts on the lifetime performance of energy harvesters. *Mechanical Systems and Signal Processing*, 156:107697, 2021.
- [20] Distributed piezoelectric actuation of a bistable buckled beam. *European Journal of Mechanics - A/Solids*, 26(5):837–853, 2007.
- [21] Christopher Rhys Bowen, Peter F. Giddings, Aki I.T. Salo, and Hyun-sun Alicia Kim. Modeling and characterization of piezoelectrically actuated bistable composites. *IEEE Transactions on Ultrasonics, Ferroelectrics, and Frequency Control*, 58(9):1737–1750, 2011.
- [22] Pedro Portela, Pedro Camanho, Paul Weaver, and Ian Bond. Analysis of morphing, multi stable structures actuated by piezoelectric patches. *Computers & Structures*, 86(3-5):347–356, 2008.
- [23] Jian Zhao, Jian Zhang, KW Wang, Kai Cheng, Hongxi Wang, Yu Huang, and Pengbo Liu. On the nonlinear snap-through of arch-shaped clamped-clamped bistable beams. *Journal of Applied Mechanics*, 87(2):024502, 2020.
- [24] Zhongwen Zhang, Li-Wei Chen, and Zhao-Dong Xu. Snap-through behavior of bistable beam with variable sections: mechanical model and experimental study. *Smart Materials and Structures*, 31(10):105004, aug 2022.
- [25] Marius Clad, Choong-Ho Rhee, and Kenn Oldham. Design and modeling of a piezoelectric, bistable out-of-plane actuator for micro-robotic appendages. In *2022 International Conference on Manipulation, Automation and Robotics at Small Scales (MARSS)*, pages 1–6, 2022.
- [26] S. Timoshenko and J.M. Gere. *Theory of Elastic Stability*. Dover Civil and Mechanical Engineering. Dover Publications, 2009.
- [27] Mattias Vangbo. An analytical analysis of a compressed bistable buckled beam. *Sensors and Actuators, A: Physical*, 69(3):212–216, 1998.
- [28] Wenzhong Yan, Yunchen Yu, and Ankur Mehta. Analytical modeling for rapid design of bistable buckled beams. *Theoretical and Applied Mechanics Letters*, 9(4):264–272, 2019.
- [29] Paul Cazottes, Amâncio Fernandes, Joël Pouget, and Moustapha Hafez. Bistable buckled beam: Modeling of actuating force and experimental validations. *Journal of Mechanical Design*, 131:101001–1–10, 2009.
- [30] Jin Qiu, Jeffrey H. Lang, and Alexander H. Slocum. A curved-beam bistable mechanism. *Journal of microelectromechanical systems*, 13(2):137–146, 2004.
- [31] Z. Chaudhry and C.A. Rogers. The pin-force model revisited. *Journal of Intelligent Material Systems and Structures*, 5:347–354, 1994.
- [32] E.F. Crawley and J. De Luis. Use of piezoelectric actuators as elements of intelligent structures. *AIAA JOURNAL*, 25:1373–1385, 1987.
- [33] Taha Ajnada, Romain Corcolle, Yves Bernard, and Laurent Daniel. Equivalent pin-forces or equivalent moments for the modelling of piezoelectric patches: a parametric study. *Engineering Research Express*, 4(2):025017, may 2022.
- [34] Xinlin P. Qing, Hian-Leng Chan, Shawn J. Beard, Teng K. Ooi, and Stephen A. Marotta. Effect of adhesive on the performance of piezoelectric elements used to monitor structural health. *International Journal of Adhesion and Adhesives*, 26(8):622–628, 2006.
- [35] C Maurini, Joel Pouget, and Stefano Vidoli. Bistable buckled beam:

modelling and piezoelectric actuation. In *Advances in Science and Technology*, volume 54, pages 281–286. Trans Tech Publ, 2008.

- [36] G.P. Gibbs and C.R. Fuller. Excitation of thin beams using asymmetric piezoelectric actuators. *Acoustical Society of America*, 89:3221–3227, 1998.
- [37] Jonathon Cleary and Hai-Jun Su. Modeling and experimental validation of actuating a bistable buckled beam via moment input. *ASME. J. Appl. Mech.*, 82(5):051005–1–7, 2015.
- [38] Hassan Hariri, Yves Bernard, and Adel Razek. A two dimensions modeling of non-collocated piezoelectric patches bonded on thin structure. *Curved and Layered Structures*, 2(1), 2014.

=2